EDGE ARTICLE

Substrate NOBINAc ligand affinity for Pd(II)-catalyzed enantioselective C−H activation over reactive β-C−H bonds in ferrocenyl amines†

Devendra Parganiha, [ID] Raviraj Ananda Thorat, [ID] Ashwini Dilip Dhumale, [ID] Yagya Dutt Upadhyay, [ID] Raushan Kumar Jha, [ID] Saravanan Raju [ID] and Sangit Kumar [ID] *

Ferrocenyl amines as directing groups for C−H activation have limitations as they are prone to undergo oxidation, allylic deamination, and β-hydride elimination. The fundamental challenge observed here is the competition between the desired C−H activation *versus* the vulnerable β-C−H bond activation of amines and fine-tuning of a suitable oxidant which avoids the oxidation of the β-C−H bond and ferrocene. Herein, the potential of an axially chiral NOBINAc ligand is revealed to implement the enantioselective Pd(II)-catalyzed C−H activation process of ferrocenyl amines. Mechanistically, the affinity between the NOBINAc ligand and sulfonate group of amine facilitated by the Cs$^+$ cation plays an impressive role in the desired reaction outcome *via* an enhanced substrate ligand affinity. This approach resulted in a Pd-catalyzed enantioselective C−H activation, the first intermolecular annulation, and alkenylation of ferrocenyl amines with allenes and olefins, leading to ferrocene fused tetrahydropyridines and alkenylated ferrocenyl amines with up to 70% yields and 99 : 1 er.

1 Introduction

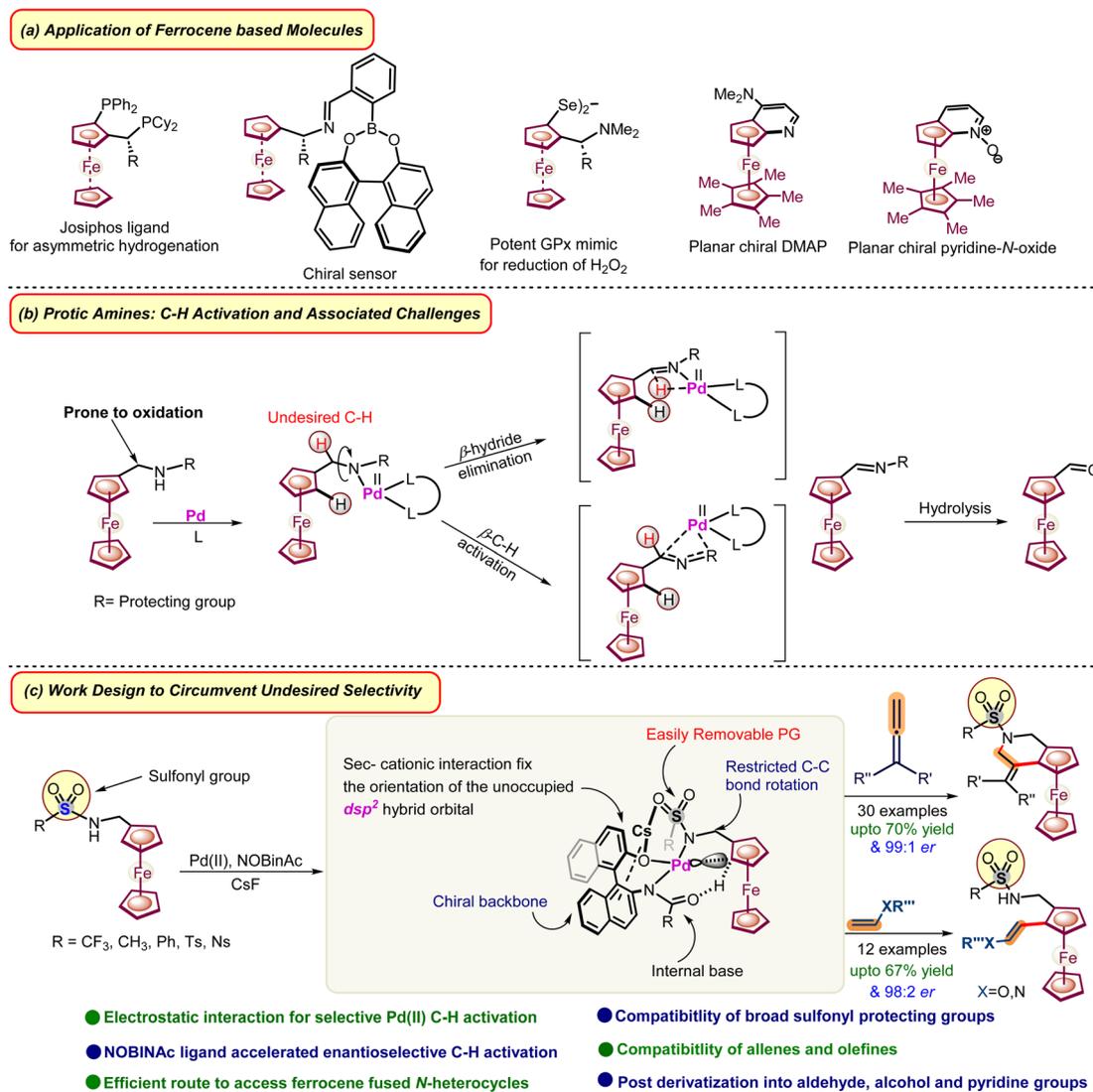The journey of ferrocene began in the 1950s, and it quickly garnered attention due to its outstanding electronic and structural characteristics.[1,2] It exhibits a highly reversible one-electron redox event and the intriguing ability to exhibit planar chirality, positioning it as an esteemed framework for asymmetric transformations in academia, industry, materials chemistry, and medicinal chemistry (Scheme 1, part a).[2] In the last few decades, ferrocene has evolved into one of the most extensively researched and developed systems for synthesizing planar chiral molecules. Consequently, several conventional organolithiums and recently developed TM-catalyzed methodologies have been employed to construct planar chiral ferrocenes.[3] However, conventional and or TM-catalyzed methodologies demand multi-step synthetic routes and oxidation-protected directing groups namely *tert*- and *sec*-amides,[4] *tert*-amines,[5] oxazolines,[6] and aldehyde.[7] This limits the construction of complex molecular architecture, as tethered directing groups[8] are difficult to remove or have difficulty

Department of Chemistry, Indian Institute of Science Education and Research Bhopal, Bhopal By-Pass Road, Bhopal, Madhya Pradesh 462066, India. E-mail: sangitkumar@iiserb.ac.in

† Electronic supplementary information (ESI) available: Synthetic procedures, reaction optimization, spectroscopic data, theoretical analysis and crystallographic information for 2347572 (R$_P$-**3a**), 2347573 (S$_P$-**3a**), and 2402043 (**3f**). CCDC 2347572, 2347573, and 2402043. For ESI and crystallographic data in CIF or other electronic format see DOI: https://doi.org/10.1039/d4sc06867j

associated with further derivatization of directing groups and requisite complex ligands for high enantioselectivity. Our group has been working on the C–H activation of ferrocene.[9] Recently, we embarked on enantioselective C–H activation strategies and preparation of chiral ferrocene molecules from ferrocene amides having an acidic proton.[9d] Enantioselective C–H activation and subsequent functionalization in the substrates having activated β-CH bonds adjacent to acidic proton containing directing groups namely –CH$_2$NHR, –CH$_2$OH, and –CH$_2$CO$_2$H are difficult as these functional groups are prone to undergo dehydrogenation, oxidation and undesired β-CH activation (Scheme 1, part b).[10] Moreover, in the case of ferrocene, it becomes more difficult to prevent oxidation as compared to other aromatics due to its lower redox potential. Therefore, conventional organo-lithiation routes or TM-catalyzed methodologies could not be employed on such substrates.3 On the other hand, ferrocene having –CH$_2$NHR groups offers numerous opportunities for complex molecular architecture. For example, these molecules can be easily annulated or readily transformed into diverse functionality after C–H activation due to the presence of reactive –CH$_2$NHR groups. Palladium catalysis offers a more accessible approach for highly enantioselective C–H activations.[11] Therefore, various ligands have been developed for Pd(II)-catalysis, solving various fundamental challenges associated with enantioselective C–H activations.[11] Here ligands play a crucial role in regulating the selectivity and expediting the C–H activation process involving various interactions.[12]

Scheme 1 Application of ferrocene–based molecules, challenges, and rational design for enabling amines as directing groups for annulation and alkenylation.

In continuation of our work on the methodology development and our long-continued interest in ferrocene,[2b,c,e] we were curious to investigate catalytic enantioselective C–H activation in the ferrocenyl amines having acidic protons which offers diverse possibilities. We envisioned that developing a Pd-catalytic pocket, with the addition of a suitable chiral ligand, could circumvent the interaction of Pd with an activated β-CH bond. Consequently, it could lead to the desired enantioselective C–H activation of ferrocenyl amines (Scheme 1, part c).

Here, we have devised a catalytic pocket by utilizing a NOBINAc ligand that underwent enantioselective C–H activation with an allene coupling partner to afford chiral ferrocene-fused pyridines with up to 99 : 1 er. Moreover, the developed Pd[II]-catalyzed C–H activation has been reacted with olefins to enable 1,2-alkenylated ferrocenyl amines up to 98 : 2 er. Control experiments and DFT calculations have also been carried out to understand the role of cation interaction in NOBINAc ligand-enabled Pd-catalyzed C–H activation.

2 Results and discussion

We initiated our study with ferrocenyl amine **1a** to explore enantioselective C–H activation by using a Pd(OAc)$_2$ catalyst, chiral ligand, and CuO oxidant in the presence of an additive CsF in THF (see Scheme 2, ESI, Tables S1–S6†).

Fascinated by the distinct regio- and chemo-divergent one to three carbon synthons possibility and further functionalization opportunity offered by allenes,[13] we set to explore allenes (**2a–2j**) as a coupling partner for enantioselective C–H activation followed by the annulation reaction. Initially, mono-protected amino acid (MPAA) ligands were tried for enantioselective C–H activation of ferrocenyl-*sec*-amine **1a** with allene **2a**. Mono-anionic (L–X) MPAA ligands **L1–L5** led to poor yield (13–16%) of annulated ferrocene fused tetrahydropyridine **3a** along with moderate 81 : 19–87 : 13 er enantioselectivity (Scheme 2). Ligand **L5** yielded the best results among ligands **L1–L5**, achieving a 14% yield and moderate 87 : 13 er (Scheme 2). Meanwhile, di-
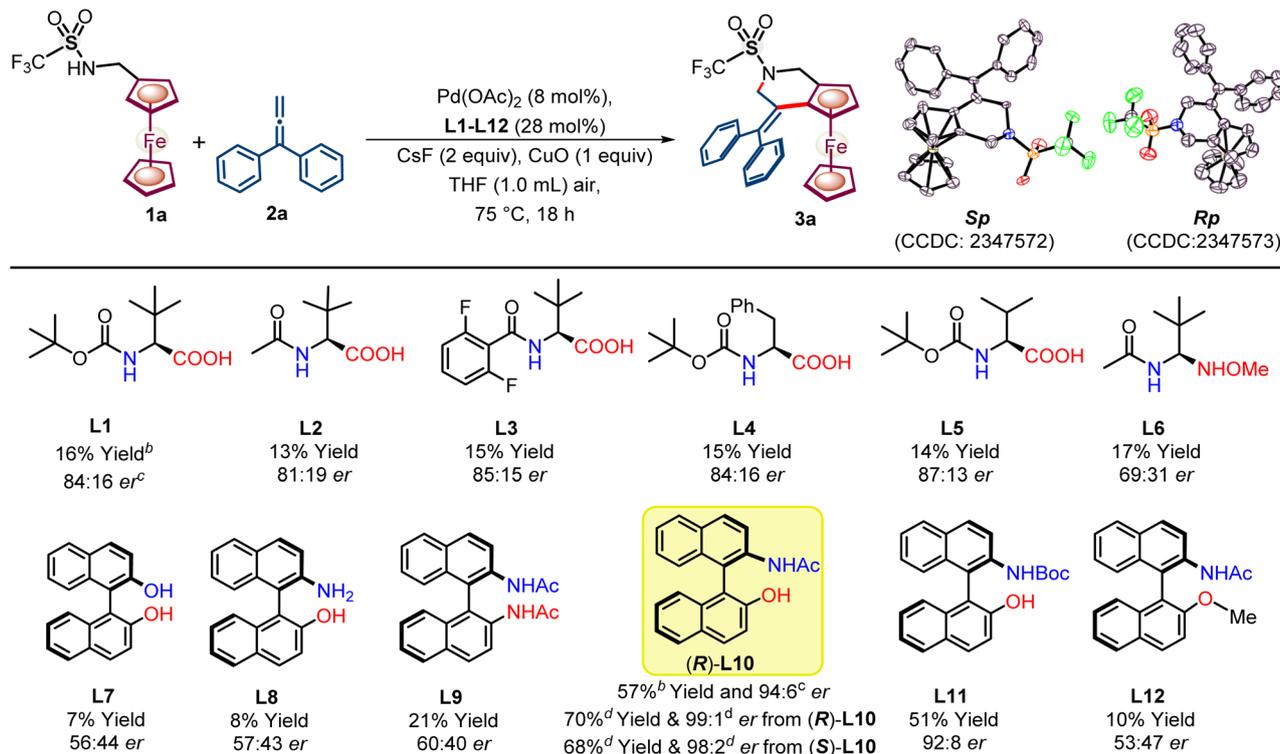
Scheme 2 Screening of the ligand and optimization of the reaction conditions. [a]Reaction conditions: **1a** (0.05 mmol), **2a** (0.1 mmol), Pd(OAc)₂ (0.004 mmol), ligand (0.014 mmol), CsF (0.1 mmol), CuO (0.05 mmol), THF (1 ml), air, T °C, 18 h. [b]Crude yield of **3a** is determined by ^{1}H NMR with CH₂Br₂ as an internal standard. [c]er of **3a** was determined by HPLC analysis. [d]Isolated yield of **3a** and enantioselectivity when the reaction was carried out in dry air.

anionic (X–X) derivatized MPAA **L6** yielded 17% of **3a** with a significant loss in enantioselectivity (69 : 31 er). Furthermore, in the presence of MPAA ligands (**L1–L6**), the excessive formation of a side product, ferrocene carboxaldehyde, was observed in the reaction, presumably due to the background oxidation and β-hydride elimination from the ferrocenyl-*sec*-amine **1a** by its undesired interaction with the Pd^{II} catalyst. Interestingly, during the screening of axially chiral binaphthyl-derived ligands **L7–L10**, NOBINAc ligand , developed by Gulias and co-workers,[12e,14] offered a good 94 : 6 er and moderate yield (57%) of ferrocene fused tetrahydropyridine **3a**. Furthermore, screening of reaction conditions by modifying NOBINAc to *N*-Boc group **L11** and NOBINAc to –OMe group **L12** afforded enantioselectivity 92 : 8 er and 53 : 47 er with low 51 and 10% yields, respectively.
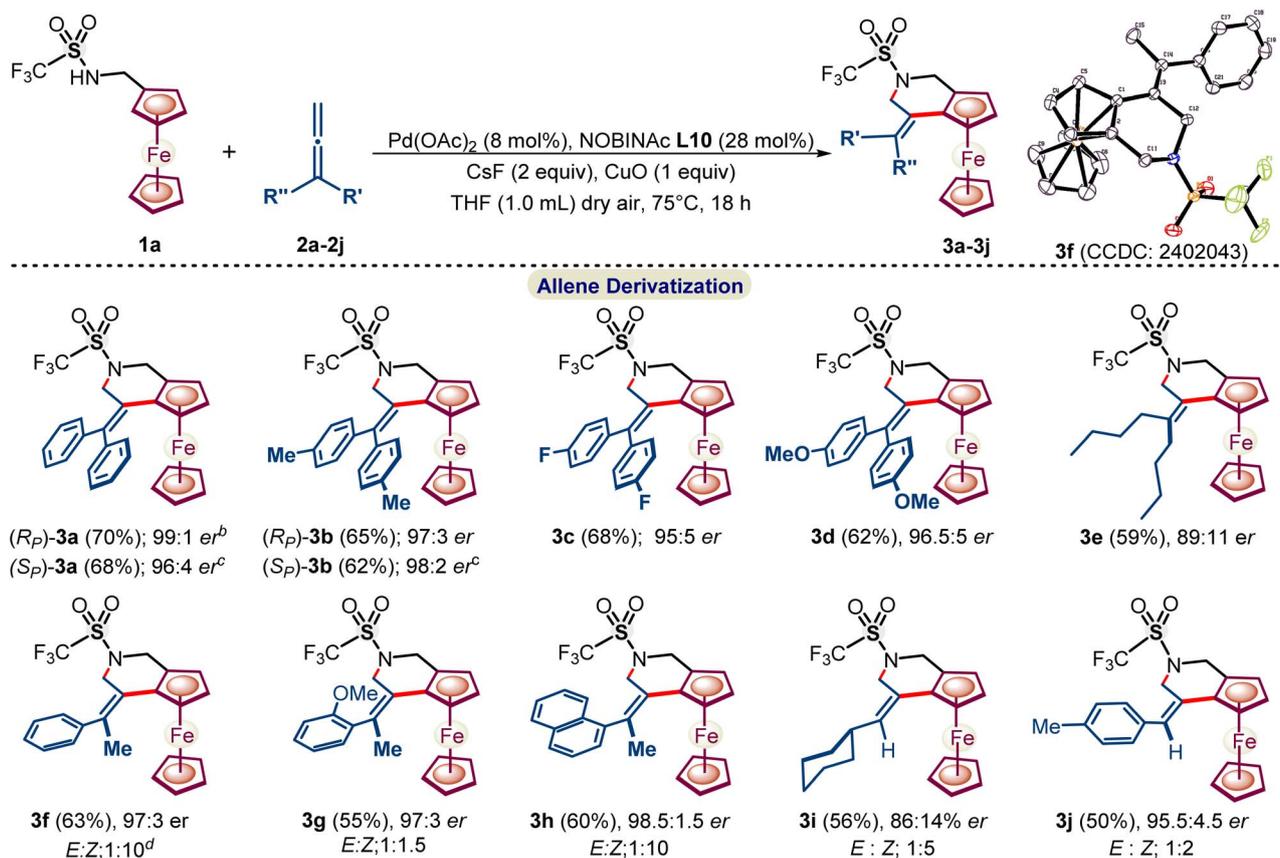
To our delight, NOBINAc ligand **L10**, under dry air atmospheric conditions, offered a 70% yield with an excellent 99 : 1 er of **3a** (see ESI, Tables S1–S5†). Moreover, using *S*-NOBINAc **L10** afforded opposite enantiomer (S$_p$)-**3a** in nearly the same yield and er. The absolute configuration of both the enantiomers of **3a** and their structures have been studied by single crystal XRD (Scheme 2). After the optimization of the reaction conditions, the applicability of the developed reaction methodology was explored regarding a variety of allenes (Scheme 3).

α,α-Diaryl substituted symmetrical allenes **2b–2d** with electron-donating and withdrawing substituents reacted

smoothly under NOBINAc **L10**-accelerated reaction conditions, leading to chiral tetrahydropyridines **3b–3d** in 62–68% yields and 95:5–99 : 1 er. Furthermore, α,α-unsymmetrical allenes **2f–2j** also underwent the enantioselective annulation reaction to afford respective tetrahydropyridines **3f–3j** in 86 : 14–97.5 : 2.5 er and better $E:Z$ selectivity up to (1 : 10) and (1 : 5), whereas substitution at the phenyl ring lowers the $E:Z$ selectivity as phenyl-substituted tetrahydropyridines **3g** and **3j** were obtained in a poor $E:Z$ up to 1 : 2. Alkyl-substituted allenes **2e** and **2i** offered alkyl-substituted tetrahydropyridines **3e** and **3i** in nearly the same yields, but with relatively lower er (89 : 11 and 86 : 14 er).

It seems that the trifluorosulfonyl (–NHTf) group not only facilitates C–H activation but also helps in preventing oxidation[15] of secondary amines through secondary cationic interactions (*vide infra*). Next, various ferrocenyl amines **1b–1f** having the possibility of potential secondary cationic interactions under the developed NOBINAc **L10** accelerated enantioselective C–H activation have been explored (Scheme 4). To our delight, ferrocenyl amines **1b–1e** having methyl, *ortho*-nitrophenyl, 3,5-difluorophenyl, and *para*-methyl-phenyl sulfonyl groups also underwent enantioselective C–H-annulation leading to diverse *N*-substituted chiral tetrahydropyridines **3k–3z** ranging yields of 28–58% with 86 : 14 to 99 : 1 er, whereas nosyl and SO₂CH₃ protected amines yielded ferrocene fused tetrahydropyridines **3t–3y** in relatively lower yields 28–42% with

Allene Derivatization

(R_P)-**3a** (70%); 99:1 er[b]
(S_P)-**3a** (68%); 96:4 er[c]

(R_P)-**3b** (65%); 97:3 er
(S_P)-**3b** (62%); 98:2 er[c]

3c (68%); 95:5 er

3d (62%), 96.5:5 er

3e (59%), 89:11 er

3f (63%), 97:3 er
$E:Z;1:10^d$

3g (55%), 97:3 er
$E:Z;1:1.5$

3h (60%), 98.5:1.5 er
$E:Z;1:10$

3i (56%), 86:14% er
$E:Z; 1:5$

3j (50%), 95.5:4.5 er
$E:Z; 1:2$

Scheme 3 Substrate scope of allene derivatization. [a]Isolated yields of **3a**–**3j** were obtained using (R)-NOBINAc unless otherwise stated. [b]er of the product was determined using an HPLC analysis. [c]er of the product obtained by using (S)-NOBINAc. [d]E : Z was determined by ^{1}H NMR.

86 : 14 er to 97 : 3 er (Scheme 4). *N*-Acetyl-protected ferrocenyl-*sec*-amine **1f** failed to afford any annulated ferrocene fused pyridine.

Furthermore, styrene and activated olefin coupling partners, which could react through π-interaction with the *in situ* formed proposed metallacycle, were also explored under the NOBINAc-accelerated reaction conditions (Scheme 5). Gratifyingly, ethyl acrylate underwent an enantioselective C–H activation reaction to provide dehydrogenative Heck-coupled ferrocenyl acrylate **4a** in 52% yield and 91 : 9 er under the optimized reaction conditions. Next, a series of substituted acrylates were coupled with ferrocenyl amines **1c** and **1d** to afford respective chiral 1,2 alkenylated ferrocenyl amines **4b–4h** in 94 : 6 to 98 : 2 er under enantioselective NOBINAc accelerated reaction conditions.

Furthermore, not only acrylates, but also *N,N*-dimethylacrylamide and dimethyl vinylphosphonate coupled enantioselectively with ferrocenyl amines to provide respective chiral 1,2-alkenylated ferrocenyl amines **4i–4j** in good 96 : 4 to 96 : 4 er, respectively. However, (vinylsulfonyl)benzene reacted sluggishly to afford traces of **4k** and unactivated styrene failed to react with ferrocenyl amine under the optimized reaction conditions.

Next, acrylate consisting of natural product moiety L-menthol and α-tocopherols reacted with excellent diastereoselectivity to afford natural product derivatized ferrocenyl amines in >20 : 1 dr. We have also tested the alkynes, phenylacetylene and 1-phenyl-1-propyne, in place of allenes as coupling partners under the optimized conditions. Phenylacetylene failed to afford any coupled product with ferrocenyl amine **1a** under the reaction conditions and 1-phenyl-1-propyne afforded only traces of the coupled product which was confirmed by mass spectrometry from the reaction mixture.
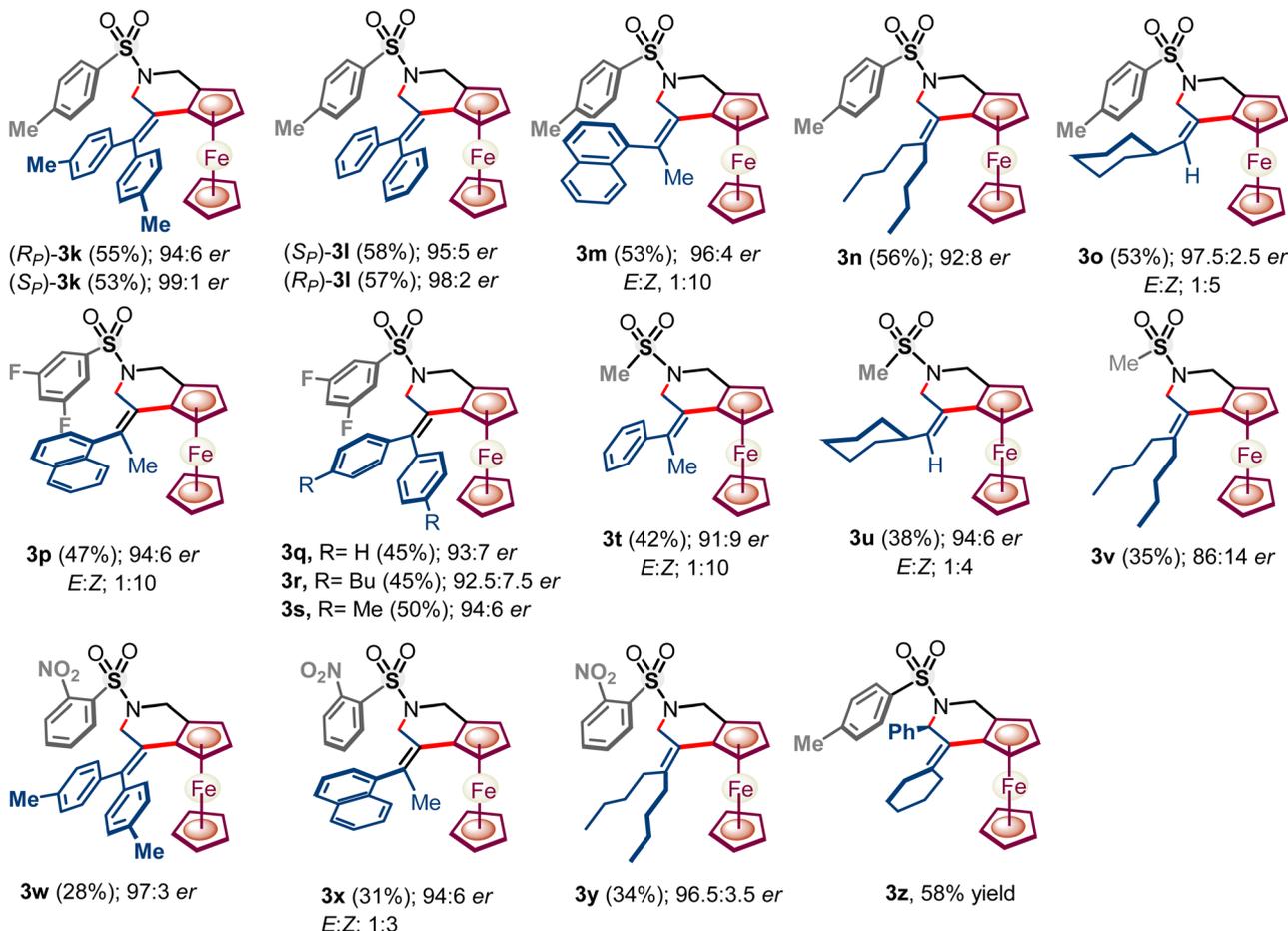
Next, we have shown that the sulfonyl protection at the amine backbone can be eliminated from synthesized chiral tetrahydropyridine **3a**, affording unprotected tetrahydropyridine **5a** with a 70% yield and 94 : 6 er (Scheme 6A).

Furthermore, amine **4b** can be readily oxidized into a versatile aldehyde group leading to chiral 1,2-alkenylated ferrocene carboxaldehyde **6a** in 55% yield and 98 : 2 er which has also been reduced into chiral ferrocenyl alcohol **7a** in 96% yield and 98 : 2 er (Scheme 6B). The utility of the synthesized chiral ferrocene fused amine **5a** has been tested as a catalyst for the enantioselective thia-Michael reaction with chalcone providing **8a** with up to 80% yield and 65 : 35 er (Scheme 6C).

2.1 Mechanistic investigation

In pursuit of an understanding of efficient work function in NOBINAc catalysis, control experiments were performed, where

(R_P)-**3k** (55%); 94:6 *er*
(S_P)-**3k** (53%); 99:1 *er*

(S_P)-**3l** (58%); 95:5 *er*
(R_P)-**3l** (57%); 98:2 *er*

3m (53%); 96:4 *er*
E:Z, 1:10

3n (56%); 92:8 *er*

3o (53%); 97.5:2.5 *er*
E:Z; 1:5

3p (47%); 94:6 *er*
E:Z; 1:10

3q, R= H (45%); 93:7 *er*
3r, R= Bu (45%); 92.5:7.5 *er*
3s, R= Me (50%); 94:6 *er*

3t (42%); 91:9 *er*
E:Z; 1:10

3u (38%); 94:6 *er*
E:Z; 1:4

3v (35%); 86:14 *er*

3w (28%); 97:3 *er*

3x (31%); 94:6 *er*
E:Z; 1:3

3y (34%); 96.5:3.5 *er*

3z, 58% yield

Scheme 4 Substrate scope with regard to ferrocenyl amines. [a]Isolated yields of **3k–3z** were obtained using (*R*)-NOBINAc unless otherwise stated. [b]er of the product was determined using an HPLC analysis. [c]er of the product obtained by using (*S*)-NOBINAc. [d]*E* : *Z* was determined by ^{1}H NMR.

the cation from the envisioned catalytic cycle was deliberately removed using water and 18-crown ether (Scheme 7). The addition of water and 18-crown ether under the standard optimized conditions shows a significant reduction in both yield and enantioselectivity [(A) conditions a and b, Scheme 7]. On the other hand, in the absence of a cation (Scheme 7A, condition c), the reaction leads to only traces of annulated product **3a** without any er.

Furthermore, other organic cationic sources exemplified by TBAF and TBAB were also tried under optimized reaction conditions; however, the reaction outcome was poor and provided nearly the same result (yields and enantioselectivity) for these organic cation sources (Scheme 7A, condition d). Additionally, NOBINAc ligand **L12** has –OH protection with a methyl group to avoid the possible cationic interaction leading to erosion of er (57 : 43 er*vs.* 98 : 2 er; Scheme 7A, condition e). This outcome indicates that the OH group is necessary for NOBINAc for an efficient work function.

Next, ^{19}F NMR was carried out on the reaction of **1a**, Pd(OAc)$_2$, NOBINAc, and various cations (Cs$_2$CO$_3$, Na$_2$CO$_3$, and Li$_2$CO$_3$). A new peak at −76.07 ppm corresponding to CF$_3$ of **1a**

emerges and increases to a maximum with the increase of the size of the cations (Li$^+$, Na$^+$, and Cs$^+$). The only mixture of Cs$_2$CO$_3$ and **1a** does not lead to any new peak in the ^{19}F NMR spectra. This may suggest that Cs$^+$ cation enhances the interaction among substrate **1a**, NOBINAc ligand **L10**, and Pd^{II} (for details, see Scheme 7B and ESI, p. S99†).

Furthermore, the rate of the reaction in the presence and absence of NOBINAc **L10** was monitored by ^{19}F NMR with respect to **3f**, which suggests that the NOBINAc **L10** accelerates the reaction by 2.2 fold (for details, see Scheme 7C and ESI, p. S101†).

Next, DFT computations were carried out to shed light on high enantioselective discrimination. The structural optimization reveals that the Cs$^+$ ion is away from the lower Cp ring in the favorable **TS1**, whereas, in unfavorable **TS2**, the Cs$^+$ ion is close to the Cp ring. A relative energy difference of 10.45 kcal mol^{-1} was realized between favorable **TS1** and unfavorable **TS2** (Scheme 7D). Thus, based on the evidence for the initial CMD step and similar previously reported literature precedence,[13e,g] a catalytic cycle has been proposed (Scheme 8).[13f,h,i] The NOBINAc ligand and ferrocenyl amine **1a** seem to undergo
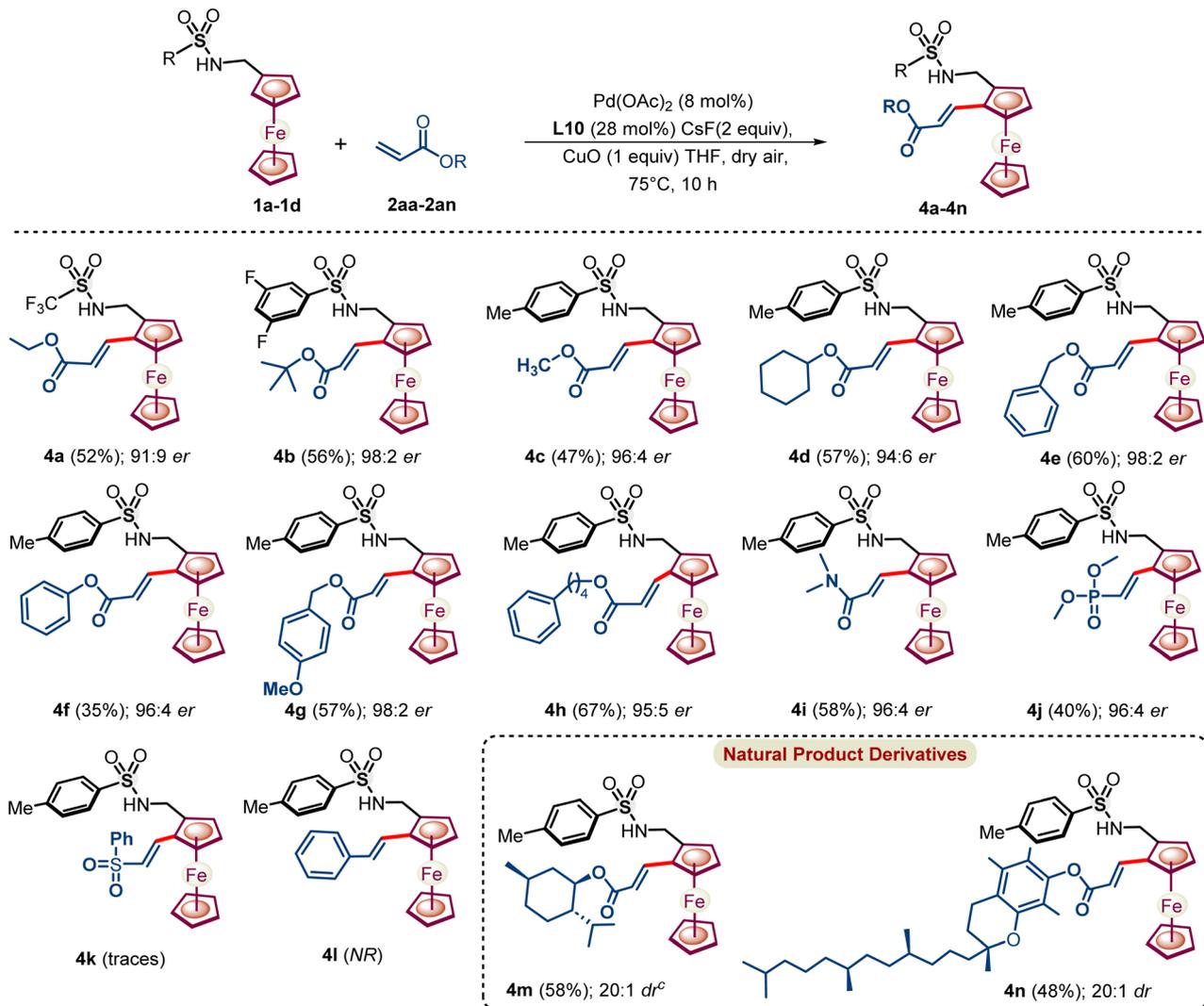
Scheme 5 Substrate scope with regard to olefins. [a]Isolated yields of **4a–4n**. [b]The er was determined by HPLC. [c]dr was determined by ^{1}HNMR.
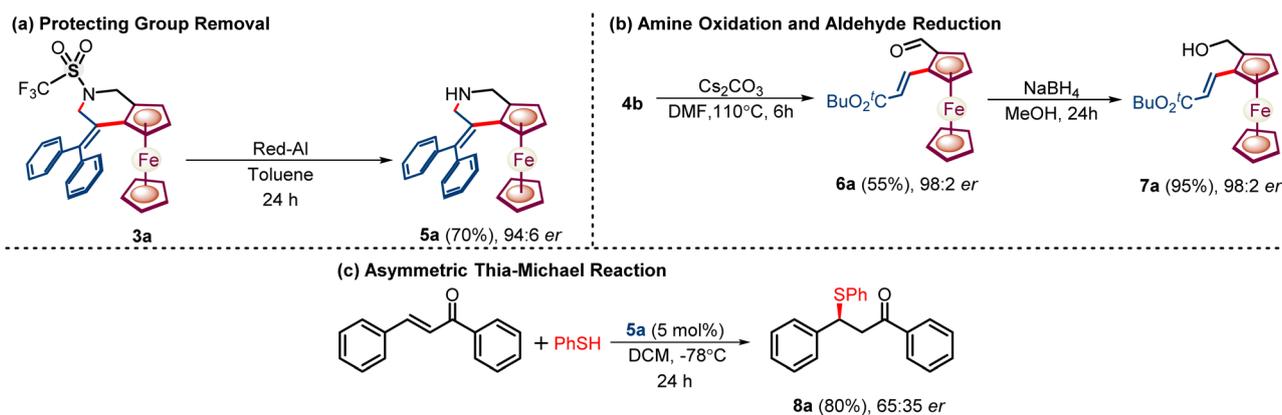

Scheme 6 Post derivatization and application of ferrocene fused chiral amine as a catalyst. Reaction conditions: (a) **3a** (0.05 mmol), red Al (0.5 mmol) in dry toluene. (b) **4b** (0.05 mmol), Cs$_2$CO$_3$ (0.1 mmol) in DMF at 110 °C for 6h. (c) Chalcone (0.1 mmol), PhSH (0.25 mmol), **5a** (0.005 mmol).
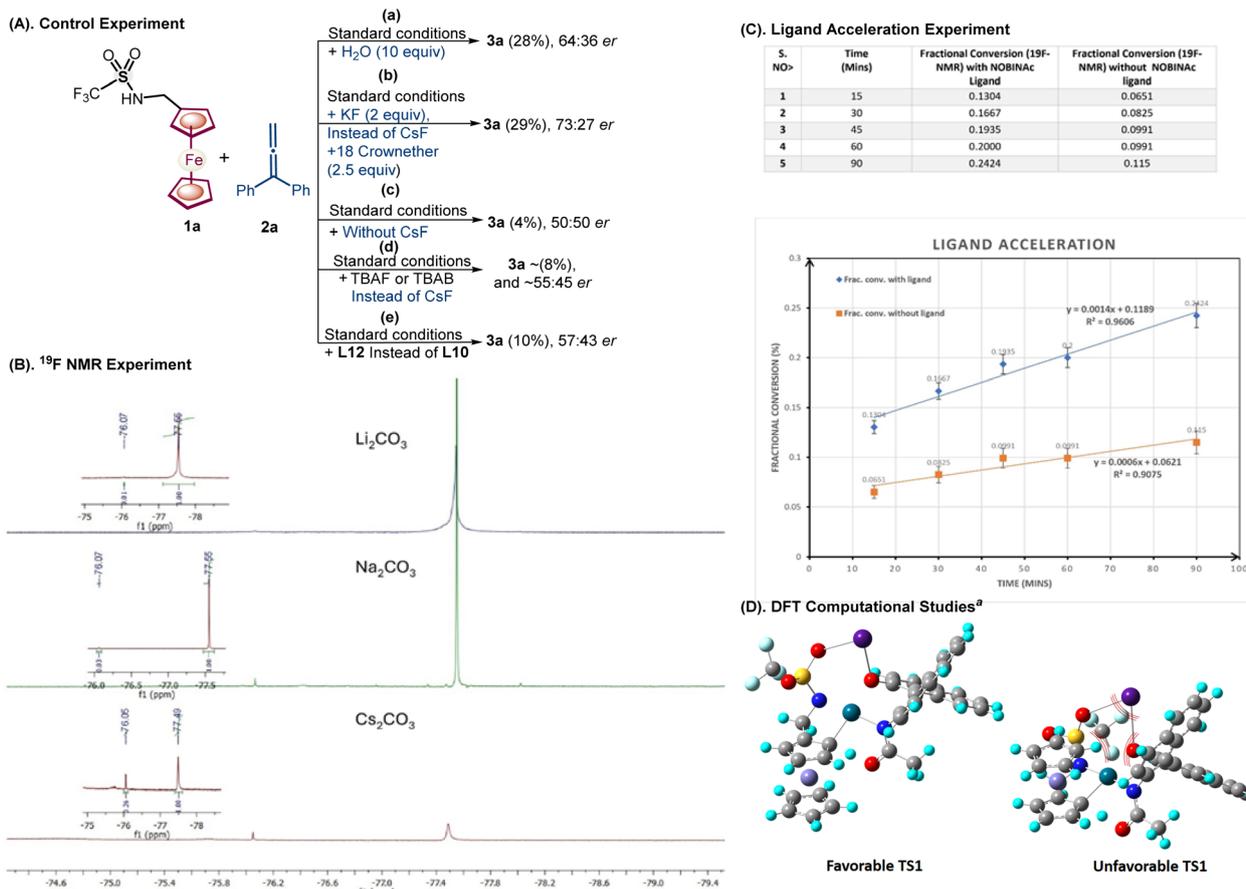
Scheme 7 Understanding of the NOBINAC work function in the presence of Cs⁺. (A) Control experiment. (B) ¹⁹F NMR experiment. (C). Ligand acceleration experiment. (D). DFT computation for favorable TS1 and unfavorable transition state TS2. ^{a}The optimization of the proposed structures derived from **1a**, Pd^{II}, S-NOBINAc, and Cs⁺ and the energies were obtained at a DFT–B3LYP/LANL2DZ level of theory (for details, see ESI, pp. S101–S111†).
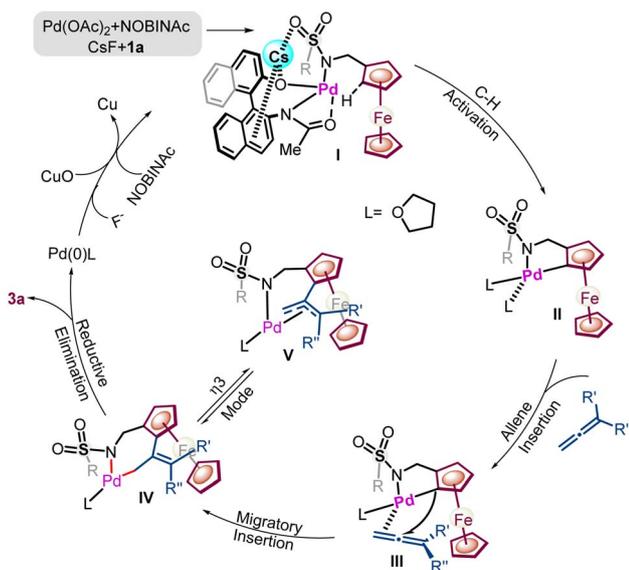
Scheme 8 Catalytic cycle for C–H annulation.

substitution with Pd(OAc)$_2$ in the presence of a CsF enabling Pd(II)amidate, which, upon the interaction of Cs⁺ with the sulfonyl group and NOBINAc, leads to the generation of a chiral catalytic pocket in palladium intermediate **I**.[12e]

Here the cationic interaction may dictate the vacant dsp^2-hybrid orbital of Pd^{II} (intermediate shown in Scheme 1) towards the desired enantiotopic C–H bond and avoid interaction with the β-C–H bond to circumvent β-hydride elimination. Furthermore, enantio-determining C–H activation occurs *via* the concerted metalation deprotonation (CMD) process which leads to palladacycle **II**.[13f] Subsequently, allene insertion takes place into palladacycle **II** to form palladacycle **III**.[13f] Furthermore, migratory insertion would lead to intermediates **IV** and **V** which upon reductive elimination could afford ferrocene fused tetrahydropyridine **3a** with concomitant release of the catalyst.[13b,f,i]

In the developed NOBINAc-catalyzed annulation reaction, Z-regioselectivity was obtained across the double bond in the ferrocenyl tetrahydropyridines. Z-selectivity over the E-regioisomer was understood by using DFT computations (Fig. 1). The optimized Z-isomer is more stable by 1.51 kcal mol^{-1} than the isolated E-regioisomer. Furthermore, palladacycle **III** seems to be the key intermediate with respect to unsymmetrical allenes to determine relative E,Z-selectivity
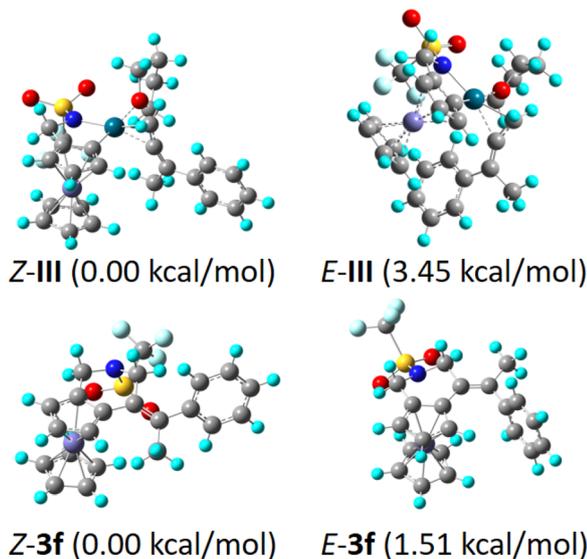
Z-**III** (0.00 kcal/mol)   E-**III** (3.45 kcal/mol)

Z-**3f** (0.00 kcal/mol)   E-**3f** (1.51 kcal/mol)

Fig. 1 DFT computation studies to determine relative Z- and E-isomer selectivity (for details, see ESI, pp. S105–S120†).

(Fig. 1). Here, the respective Z-intermediate in which the phenyl substituent of unsymmetrical allene is away from the C_P ring shows lower energy by 3.45 kcal mol^{-1} than the respective E-intermediate (Fig. 1).

3 Conclusion

In summary, we have addressed a fundamental problem associated with amine substrates having activated β-CH bonds adjacent to the acidic proton (–CH$_2$NH̲R) for the desired enantioselective CH activation by a meticulously designed Pd-catalytic pocket. Here, the NOBINAc ligand and ferrocenyl amine enable Pd^{II}-catalyzed highly enantioselective C–H activation. Furthermore, it has been observed that the amines having sulfonyl groups are crucial for high enantioselective induction. The subsequent annulation and alkenylation enable the development of an efficient methodology for synthesizing chiral ferrocene-fused tetrahydropyridine and 2-alkenylated ferrocenyl amines. The sulfonyl-protecting group can be effortlessly removed to provide chiral ferrocenyl amine, which shows the application as a chiral catalyst. Similarly, 2-alkenylated ferrocenyl amine has been oxidized into respective ferrocene carboxaldehyde which is a versatile group for further derivatization into alcohols. So far the initial results have allowed us to explore the introduction of coupling partners within allenes and acrylates. Future investigations are underway to explore the feasibility of introducing coupling partners through transmetallation or oxidative addition, enabling ferrocenyl amine-derived arylation and heteroatom insertion reactions.

Data availability

Detailed synthetic procedures, reaction condition optimization, data characterization, controlled experiments, X-ray diffraction

structural analyses, and geometries and energies of theoretically investigated structures have been provided in the ESI.†

Author contributions

SK and DP wrote the manuscript. DP, ADD, YDU, and RT performed synthesis and characterization. DP has performed controlled experiments. RJ and SR performed DFT computations. All authors have approved the final version of the manuscript.

Conflicts of interest

There are no conflicts to declare.

Acknowledgements

Notes and references

1 (a) T. J. Kealy and P. L. Pauson, *Nature*, 1951, **168**, 1039–1040; (b) G. Wilkinson, M. Rosenblum, M. C. Whiting and R. B. Woodward, *J. Am. Chem. Soc.*, 1952, **74**, 2125–2126.

2 (a) G. Mugesh, A. Panda, H. B. Singh, N. S. Punekar and R. J. Butcher, *J. Am. Chem. Soc.*, 2001, **123**, 839–850; (b) G. Mugesh, A. Panda, S. Kumar, S. D. Apte, H. B. Singh and R. J. Butcher, *Organometallics*, 2002, **21**, 884; (c) S. Kumar, H. B. Singh and G. Wolmershauser, *Organometallics*, 2006, **25**, 382; (d) T. Muraoka, K. Kinbara and T. Aida, *Nature*, 2006, **440**, 512–515; (e) S. Kumar, J.-C. P. Helt, J. Autschbach and M. R. Detty, *Organometallics*, 2009, **28**, 3426; (f) G. Mirri, S. D. Bull, P. N. Horton, T. D. James, L. Male and J. H. R. Tucker, *J. Am. Chem. Soc.*, 2010, **132**, 8903–8905; (g) D. Astruc, *Eur. J. Inorg. Chem.*, 2017, **2017**, 6–29; (h) M. Patra and G. Gasser, *Nat. Rev. Chem.*, 2017, **1**, 0066; (i) O. Bernardo, S. G. Pelayo and L. A. López, *Eur. J. Inorg. Chem.*, 2022, **2022**, e202100911.

3 (a) M. Tsukazaki, A. Roglans, B. J. Chapell, N. J. Taylor and V. Snieckus, *J. Am. Chem. Soc.*, 1996, **118**, 685 (more references therein on ortho-lithiation).; (b) Z.-J. Cai, C.-X. Liu, Q. Wang, Q. Gu and S.-L. You, *Nat. Commun.*, 2019, **10**, 4168–4175; (c) S. R. Yetra, Z. Shen, H. Wang and L. Ackermann, *Beilstein J. Org. Chem.*, 2018, **14**, 1546–1553; (d) C. X. Liu, Q. Gu and S.-L. You, *Trends Chem.*, 2020, **2**, 737–749; (e) Z.-Z. Zhang, D.-Y. Huang and B.-F. Shi, *Org. Biomol. Chem.*, 2022, **20**, 4061–4073; (f) P. Dolui, A. Verma and A. J. Elias, *Directing Group-Assisted C-H Functionalization of Ferrocene and CpCo(C$_4$Ph$_4$) Derivatives*, Wiley-VCH, 2022, DOI: 10.1002/9783527834242.chf0074; (g)

C.-X. Liu, P.-P. Xie, F. Zhao, Q. Wang, Z. Feng, H. Wang, C. Zheng and S.-L. You, *J. Am. Chem. Soc.*, 2023, **145**, 4765–4773; (*h*) C.-X. Liu, F. Zhao, Z. Feng, Q. Wang, Q. Gu and S.-L. You, *Nat. Synth.*, 2023, **2**, 49–57; (*i*) T. Carny and R. Sebesta, *Synlett*, 2024, **35**, 165–182.

4 (*a*) Q. Wang, Y. H. Nie, C. X. Liu, W. W. Zhang, Z. J. Wu, Q. Gu, C. Zheng and S.-L. You, *ACS Catal.*, 2022, **12**, 3083–3093; (*b*) Q.-J. Yao, F.-R. Huang, J.-H. Chen and B.-F. Shi, *Nat. Commun.*, 2024, **15**, 7135.

5 (*a*) D. W. Gao, Q. Gu and S.-L. You, *J. Am. Chem. Soc.*, 2016, **138**, 2544–2547; (*b*) Z. J. Cai, C. X. Liu, Q. Gu, C. Zheng and S.-L. You, *Angew. Chem., Int. Ed.*, 2019, **58**, 2149–2153; (*c*) L. Zhou, H. G. Cheng, L. Li, K. Wu, J. Hou, C. Jiao, S. Deng, Z. Liu, J. Q. Yu and Q. Zhou, *Nat. Chem.*, 2023, **15**, 815–823.

6 (*a*) W.-J. Kong, Q. Shao, M.-H. Li, Z.-L. Zhou, H. Xu, H.-X. Dai and J.-Q. Yu, *Organometallics*, 2018, **37**, 2832–2836; (*b*) X. Kuang, J.-J. Li, T. Liu, C.-H. Ding, K. Wu, P. Wu and J.-Q. Yu, *Nat. Commun.*, 2023, **14**, 7698.

7 C.-X. Liu, F. Zhao, Q. Gu and S.-L. You, *ACS Cent. Sci.*, 2023, **9**, 2036–2043.

8 Reference for tethered directing groups:(*a*) M. Ogasawara, S. Watanabe, K. Nakajima and T. Takahashi, *J. Am. Chem. Soc.*, 2010, **132**, 2136–2137; (*b*) D. W. Gao, Q. Yin, Q. Gu and S.-L. You, *J. Am. Chem. Soc.*, 2014, **136**, 4841–4844.

9 (*a*) M. Sattar and S. Kumar, *Org. Lett.*, 2017, **19**, 5960–5963; (*b*) R. A. Thorat, S. Jain, M. Sattar, P. Yadav, Y. Mandhar and S. Kumar, *J. Org. Chem.*, 2020, **85**, 14866–14878 (other related references therein).; (*c*) R. A. Thorat, Y. Mandhar, D. Parganiha, K. B. Patil, V. Singh, B. Shakir, S. Raju and S. Kumar, *ChemistrySelect*, 2023, **8**, e202203945; (*d*) R. A. Thorat, D. Parganiha, S. Jain, V. Choudhary, B. Shakir, K. Rohilla, R. K. Jha and S. Kumar, *ChemRxiv*, 2023, preprint, DOI: 10.26434/chemrxiv-2023-918dp-v3.

10 (*a*) P. L. Theofanis and W. A. Goddard, *Organometallics*, 2011, **30**, 4941–4948; (*b*) M. B. Li, Y. Wang and S. K. Tian, *Angew. Chem., Int. Ed.*, 2012, **51**, 2968–2971; (*c*) Z. Zhuang and J.-Q. Yu, *J. Am. Chem. Soc.*, 2020, **142**, 12015–12019; (*d*) V. G. Landge, A. J. Grant, Y. Fu, A. M. Rabon, J. L. Payton and M. C. Young, *J. Am. Chem. Soc.*, 2021, **143**, 10352–10360; (*e*) Y. Sekiguchi, J. H. Pang, J. S. Ng, J. Chen, K. Watanabe, R. Takita and S. Chiba, *JACS Au*, 2022, **2**, 2758–2764; (*f*) R. Keshri, D. Rana, A. Saha, S. A. Al-Thabaiti, A. A. Alshehri, S. M. Bawaked and D. Maiti, *ACS Catal.*, 2023, **13**, 4500–4516; (*g*) D. A. Strassfeld, C. Y. Chen, H. S. Park, D. Q. Phan and J.-Q. Yu, *Nature*, 2023, **622**, 80–86.

11 (*a*) B.-F. Shi, N. Maugel, Y. H. Zhang and J.-Q. Yu, *Angew. Chem., Int. Ed.*, 2008, **47**, 4882–4886; (*b*) D. W. Gao, Y. C. Shi, Q. Gu, Z. L. Zhao and S.-L. You, *J. Am. Chem. Soc.*, 2013, **135**, 86–89; (*c*) L. Chu, K. J. Xiao and J.-Q. Yu, *Science*, 2014, **346**, 451–455; (*d*) Q. J. Yao, P. P. Xie, Y. J. Wu, Y. L. Feng, M. Y. Teng, X. Hong and B.-F. Shi, *J.*

Am. Chem. Soc., 2020, **142**, 18266–18276; (*e*) B. B. Zhan, L. Jin and B.-F. Shi, *Trends Chem.*, 2022, **4**, 220–235; (*f*) X. Lv, M. Wang, Y. Zhao and Z. Shi, *J. Am. Chem. Soc.*, 2024, **146**, 3483–3491.

12 (*a*) G. Meng, N. Y. S. Lam, E. L. Lucas, T. G. S. Denis, P. Verma, N. Chekshin and J.-Q. Yu, *J. Am. Chem. Soc.*, 2020, **142**, 10571–10591; (*b*) G. R. Genov, J. L. Douthwaite, A. S. K. Lahdenpera, D. C. Gibson and R. J. Phipps, *Science*, 2020, **367**, 1246–1251; (*c*) U. Dutta, S. Maiti, T. Bhattacharya and D. Maiti, *Science*, 2021, **372**, eabd5992; (*d*) Y. Lou, J. Wei, M. Li and Y. Zhu, *J. Am. Chem. Soc.*, 2022, **144**, 123–129; (*e*) J. M. González, X. Vidal, M. A. Ortuño, J. L. Mascareñas and M. Gulías, *J. Am. Chem. Soc.*, 2022, **144**, 21437–21442; (*f*) L. Hu, G. Meng, X. Chen, J. S. Yoon, J. R. Shan, N. Chekshin, D. A. Strassfeld, T. Sheng, Z. Zhuang, R. Jazzar, G. Bertrand, K. N. Houk and J.-Q. Yu, *J. Am. Chem. Soc.*, 2023, **145**, 16297–16304; (*g*) N. Goswami, S. K. Sinha, P. Mondal, S. Adhya, A. Datta and D. Maiti, *Chem*, 2023, **9**, 989–1003; (*h*) M. Kadarauch, D. M. Whalley and R. J. Phipps, *J. Am. Chem. Soc.*, 2023, **145**, 25553–25558; (*i*) K. Wu, N. Lam, D. A. Strassfeld, Z. Fan, J. X. Qiao, T. Liu, D. Stamos and J.-Q. Yu, *Angew. Chem., Int. Ed.*, 2024, **63**, e202400509.

13 (*a*) S. Nakanowatari, T. Muller, J. C. A. Oliveira and L. Ackermann, *Angew. Chem., Int. Ed.*, 2017, **56**, 15891–15895; (*b*) B. Cendo, N. Casanova, C. Comanescu, R. G. Fandin, A. Seoane, M. Gulías and J. L. Mascarenas, *Org. Lett.*, 2017, **19**, 1674–1677; (*c*) R. Santhoshkumar and C.-H. Cheng, *Asian J. Org. Chem.*, 2018, **7**, 1151–1163; (*d*) J. Mo, T. Müller, J. C. A. Oliveira and L. Ackermann, *Angew. Chem., Int. Ed.*, 2018, **57**, 7719–7723; (*e*) C. Zhu, J. L. Schwarz, S. Cembellín, S. Greßies and F. Glorius, *Angew. Chem., Int. Ed.*, 2018, **57**, 437–441; (*f*) X. Vidal, J. L. Mascareñas and M. Gulías, *J. Am. Chem. Soc.*, 2019, **141**, 1862–1866; (*g*) J. P. Schmidt and B. Breit, *Angew. Chem., Int. Ed.*, 2020, **59**, 23485–23490; (*h*) J. M. González, B. Cendón, J. L. Mascareñas and M. Gulías, *J. Am. Chem. Soc.*, 2021, **143**, 3747–3752; (*i*) X. Vidal, J. L. Mascarenas and M. Gulías, *Org. Lett.*, 2021, **23**, 5323–5328; (*j*) F. Panahi, F. Bauer and B. Breit, *Acc. Chem. Res.*, 2023, **56**, 3676–3693; (*k*) Y. Xu, Y. Lin, S. L. Homölle, J. C. A. Oliveira and L. Ackermann, *J. Am. Chem. Soc.*, 2024, **146**, 24105–24113; (*l*) F. Panahi and B. Breit, *Angew. Chem., Int. Ed.*, 2024, **63**, e202317981.

14 (*a*) P. Losada, L. Goicoechea, J. L. Mascarenas and M. Gulias, *ACS Catal.*, 2023, **13**, 13994–13999; (*b*) D. H. Dethe, V. Kumar and M. Shukla, *Chem. Sci.*, 2023, **14**, 11267–11272.

15 S. Feng, M. Huang, J. R. Lamb, W. Zhang, R. Tatara, Y. Zhang, Y. G. Zhu, C. F. Perkinson, J. A Johnson and Y. S. Horn, *Chem*, 2019, **5**, 2630–2641.